© 2015. Published by The Company of Biologists Ltd | Development (2015) 142, 196-206 doi:10.1242/dev.112714

RESEARCH ARTICLE

Enthesis fibrocartilage cells originate from a population of Hedgehog-responsive cells modulated by the loading environment

Andrea G. Schwartz[1], Fanxin Long[1,2,3] and Stavros Thomopoulos[1,4,5,*]

ABSTRACT

Tendon attaches to bone across a specialized tissue called the enthesis. This tissue modulates the transfer of muscle forces between two materials, i.e. tendon and bone, with vastly different mechanical properties. The enthesis for many tendons consists of a mineralized graded fibrocartilage that develops postnatally, concurrent with epiphyseal mineralization. Although it is well described that the mineralization and development of functional maturity requires muscle loading, the biological factors that modulate enthesis development are poorly understood. By genetically demarcating cells expressing Gli1 in response to Hedgehog (Hh) signaling, we discovered a unique population of Hh-responsive cells in the developing murine enthesis that were distinct from tendon fibroblasts and epiphyseal chondrocytes. Lineage-tracing experiments revealed that the Gli1 lineage cells that originate *in utero* eventually populate the entire mature enthesis. Muscle paralysis increased the number of Hh-responsive cells in the enthesis, demonstrating that responsiveness to Hh is modulated in part by muscle loading. Ablation of the Hh-responsive cells during the first week of postnatal development resulted in a loss of mineralized fibrocartilage, with very little tissue remodeling 5 weeks after cell ablation. Conditional deletion of smoothened, a molecule necessary for responsiveness to Ihh, from the developing tendon and enthesis altered the differentiation of enthesis progenitor cells, resulting in significantly reduced fibrocartilage mineralization and decreased biomechanical function. Taken together, these results demonstrate that Hh signaling within developing enthesis fibrocartilage cells is required for enthesis formation.

KEY WORDS: Biomineralization, Fibrocartilage, Indian hedgehog, Lineage tracing, Postnatal development, Tendon enthesis, Mouse

INTRODUCTION

The attachment sites of tendon to bone, termed entheses, are adapted to transfer muscle forces from tendon to bone. This specialized tissue limits stress concentrations that arise at the interface between the two mechanically disparate materials via gradients in structure and composition (Lu and Thomopoulos, 2013; Thomopoulos et al., 2010). Entheses are broadly classified into two groups based on their morphology (Benjamin et al., 2002; Wang et al., 2013). Fibrous entheses include a periosteal component and typically insert into the metaphyses or diaphyses of long bones. By contrast, fibrocartilagenous attachments typically insert into epiphyses or bone ridges. These attachments are characterized by a partially mineralized region of fibrocartilage at the tendon-bone interface, with a round cell morphology and increased proteoglycan content relative to tendon (Schwartz et al., 2012). Due to these characteristics, mature entheses have been likened to arrested growth plates (Thomopoulos et al., 2010).

Indian hedgehog (Ihh), one of three Hedgehog (Hh) family members in mammals, has been well characterized in developing bone and is known to play a crucial role in endochondral bone formation (Kronenberg, 2003; Long and Ornitz, 2013). In the growth plate, Ihh regulates the pace of chondrocyte maturation through a negative-feedback loop with parathyroid hormone-related protein (PTHrP; also known as Pthlh – Mouse Genome Informatics) (Lanske et al., 1996; Vortkamp et al., 1996). Ihh, which is expressed by pre-hypertrophic and hypertrophic chondrocytes, induces expression of PTHrP in periarticular chondrocytes away from the Ihh-producing domain, which in turn represses chondrocyte maturation. Hh proteins act in a paracrine fashion on cells through the cell surface transmembrane proteins patched (Ptch) and smoothened (Smo). In the absence of Hh, Ptch inhibits Smo signaling, allowing members of the Gli transcription factor family to suppress downstream genes. Binding of Hh to Ptch relieves the inhibition of Smo, which translocates to the primary cilia and activates Gli-dependent downstream target genes such as *Ptch* (*Ptch1*) and *Gli1* (Ingham and McMahon, 2001; Lai and Mitchell, 2005; Wang et al., 2009). Ihh expression is influenced by cyclic mechanical stress in chondrocyte cultures (Wu et al., 2001). A more recent study correlated Ihh expression with levels of mechanical forces in intact embryonic bones (Nowlan et al., 2008).

The development of fibrocartilage in the enthesis occurs postnatally, concurrently and in close proximity to epiphyseal mineralization of the humeral head (Schwartz et al., 2012). Fibrocartilage is not evident at the enthesis of mouse rotator cuffs until 2-3 weeks after birth (Galatz et al., 2007). Recently, factors associated with the Hh pathway have been localized to various entheses. PTHrP is widely expressed in numerous fibrous entheses and deletion of PTHrP results in bony outgrowths (Wang et al., 2013). Additionally, expression levels of this molecule depend on the loading environment (Chen et al., 2007; Wang et al., 2013). Expression of Gli1, a transcriptional effector and a direct target gene of all Hh proteins, has also been identified in fibrocartilagenous entheses (Blitz et al., 2009; Liu et al., 2012). Based on these findings, it was hypothesized in the current study that Hh signaling contributes to enthesis development and maintenance.

We identified Hh-responsive cells and their progenies in the late embryonic and postnatal enthesis using a lineage-tracing

[1]Department of Orthopaedic Surgery, Washington University in St Louis, St Louis, MO 63110, USA. [2]Department of Medicine, Washington University in St Louis, St Louis, MO 63110, USA. [3]Department of Developmental Biology, Washington University in St Louis, St Louis, MO 63110, USA. [4]Department of Biomedical Engineering, Washington University in St Louis, St Louis, MO 63110, USA. [5]Department of Mechanical Engineering & Materials Science, Washington University in St Louis, St Louis, MO 63110, USA.

*Author for correspondence (ThomopoulosS@wudosis.wustl.edu)

Received 22 May 2014; Accepted 7 November 2014

Development (2015) 142, 196-206 doi:10.1242/dev.112714

approach. We then showed that Ihh signaling and the size of this cell population are modulated by the loading environment. Cell ablation experiments demonstrated that this precursor cell population is necessary for the development and maintenance of partially mineralized fibrocartilage in the enthesis. Finally, we showed that active Hh signaling in this cell population is required for the proper mineralization and biomechanical properties of the tendon enthesis.

RESULTS

Enthesis fibrocartilage cells are derived from a unique population of Hh-responsive cells

To begin to address a potential role of Hh signaling in enthesis development, we monitored Hh activity using the *Gli1-Cre^{ERT2}* mouse strain that expresses tamoxifen (TAM)-inducible Cre activity (*Cre^{ERT2}*) from the *Gli1* genomic locus (Ahn and Joyner, 2004). Expression of this construct has been shown to be modulated by Hh signaling (Shin et al., 2011; Zhao et al., 2014). Specifically, *Gli1-Cre^{ERT2}* mice were crossed with Cre reporter mT/mG mice to generate progenies harboring one copy of each allele (hereafter *Gli1-Cre^{ERT2};mTmG* mice) (Muzumdar et al., 2007). Others have indicated that, following injection, TAM remains active for ∼36 h in the mouse (Ahn and Joyner, 2004). Therefore, to identify cells actively responding to Hh signals, we injected the *Gli1-Cre^{ERT2};mTmG* mice with TAM at various time points and harvested them after 2-4 days (Fig. 1A-H). Cells from these mice displayed membrane-associated red fluorescence (mTomato), except for Hh-responsive (Gli1-expressing) cells, where the red fluorescence was replaced by green fluorescence (mGFP). Hh-responsive cells were detected in the postnatal supraspinatus enthesis, consistent with previous reports for other entheses (Blitz et al., 2009; Liu et al., 2012; Wang et al., 2006). The Gli1-expressing cells were present at E16.5 when TAM was injected at E14.5, and at the immature tendon-to-bone interface at P0 with E16.5 TAM injection (Fig. 1A,B). At P1 with E18.5 TAM injection, Gli1-positive cells were seen in a narrow zone between tendon and the epiphyseal cartilage (Fig. 1C). The Gli1-expressing cells were arranged in columns and had a round morphology, characteristic of chondrocytes, and distinct from that of spindle-shaped tendon fibroblasts (supplementary material Fig. S1). They appeared to be distinct from the epiphyseal chondrocytes underlying the tendon attachment (Fig. 1A-H, dotted line). Gli1-expressing cells were evident in the enthesis, perichondrium and growth plate from E14.5-E17.5 (supplementary material Fig. S2). During late embryonic development, cells within the developing articular surface downregulated Gli1, whereas expression in the enthesis persisted.

At P8, the secondary ossification center was evident in the humeral head and two distinct populations of Gli1-expressing cells were observed near the developing enthesis (Fig. 1E). One population was more abundant, corresponding to that observed at birth at the tendon-epiphyseal cartilage interface (Fig. 1E, yellow arrowhead). A second, distinct population was separated from the first by a band of non-mineralized epiphyseal chondrocytes, and corresponded to chondrocytes adjacent to the mineralization front within the secondary ossification center (Fig. 1E, white arrowhead). By P15 (Fig. 1F), a single Gli1-expressing cell population was observed in the enthesis spanning the developing fibrocartilage. Gli1 expression persisted throughout the thickness of the fibrocartilage zone through P29 (Fig. 1G). By P56 (Fig. 1H), the Gli1-expressing cell population was limited to non-mineralized areas. These results illustrate that a cell population within the enthesis is responsive to Hh throughout postnatal development. However, whereas the Hh-responsive cells initially populated the entire fibrocartilage region, they became limited to the non-mineralized fibrocartilage in mature entheses.

The source of the Hh ligand driving Gli1 expression in the enthesis remains unclear. Ihh is a likely source as it has been shown to act on other epiphyseal cell types throughout bone development (St-Jacques et al., 1999; Vortkamp et al., 1996, 1998). Although Ihh expression was primarily limited to the primary ossification center in neonatal mice, Ihh was expressed in the secondary ossification center near the enthesis during the first week of postnatal development (supplementary material Fig. S3) (Vortkamp et al., 1998). *In situ* hybridization revealed that *Ihh* was expressed in the secondary ossification center by P7 and remained detectable at P21, albeit at lower levels (supplementary material Fig. S3B,C). However, during the first week of postnatal development, the mineralization front of the secondary ossification center has not yet reached the Hh-responsive cell population at the enthesis (Schwartz et al., 2012). The source of Ihh for the enthesis at this time might therefore be the pre-hypertrophic chondrocytes within the secondary ossification center (supplementary material Fig. S3B). By P28, the fibrocartilage zone is mineralized (Schwartz et al., 2012), yet most of the cells in the mineralized and non-mineralized zones remain Hh responsive (Fig. 1G). At this point, Ihh may originate from the secondary ossification center and exert long-range signaling to the enthesis (supplementary material Fig. S3C).

In order to determine the fate of Gli1-expressing cells within the developing enthesis, we performed lineage-tracing experiments. Mice were sacrificed at an extended period of time (e.g. 2 or 4 months) after TAM injection. Cells identified as Gli1 positive at P6 (Fig. 1E) spanned the entire region of fibrocartilage by P56 and P112, indicating that all cells in mature fibrocartilage were derived from Gli1-positive cells (Fig. 1I,M). This was also true of the developing Achilles tendon and anterior cruciate ligament entheses (Fig. 1N,O). However, these Gli1-positive cells were not labeled in a parallel experiment with *Col2-Cre™;mTmG* mice, and thus represent a distinct population from the epiphyseal chondrocytes of the neonatal humeral head (Fig. 2). Cells identified as Gli1 positive when labeled at P13 (Fig. 1F) also followed a similar pattern at P56 (Fig. 1J). When cells were labeled at P26, a narrow band of unlabeled cells parallel to the tendon-bone interface was evident between the labeled cells and the underlying bone (Fig. 1K). This gap progressively increased in width as cells were labeled at later developmental stages (Fig. 1L,H; TAM injection at P42 and P52, respectively). This suggests that only a subset of the original Hh-responsive cell population restricted to the non-mineralized side of the insertion remained Hh responsive as the animal matured. Notably, most progenies from the early Hh-responsive cells remained in the enthesis but were no longer responsive to Hh as the skeleton matured.

The lineage-tracing experiments suggest that a distinct cell population, which begins to differentiate early in perinatal development, is responsible for populating and maintaining the mature enthesis fibrocartilage. The number and density of Gli1-positive cells in the enthesis increased by more than 100% between P7 and P56 (Fig. 1P). In order to understand how a small initial cell population (Fig. 1E) could populate the entire fibrocartilage region of the mature enthesis, we assayed for cell proliferation within the enthesis. Using EdU, a thymidine analog that is incorporated into DNA during S phase of the cell cycle, we selectively labeled rapidly proliferating cells *in vivo* and compared these with the Hh-responsive cell population found in the enthesis throughout postnatal development. Few rapidly proliferating cells were

Development (2015) 142, 196-206 doi:10.1242/dev.112714

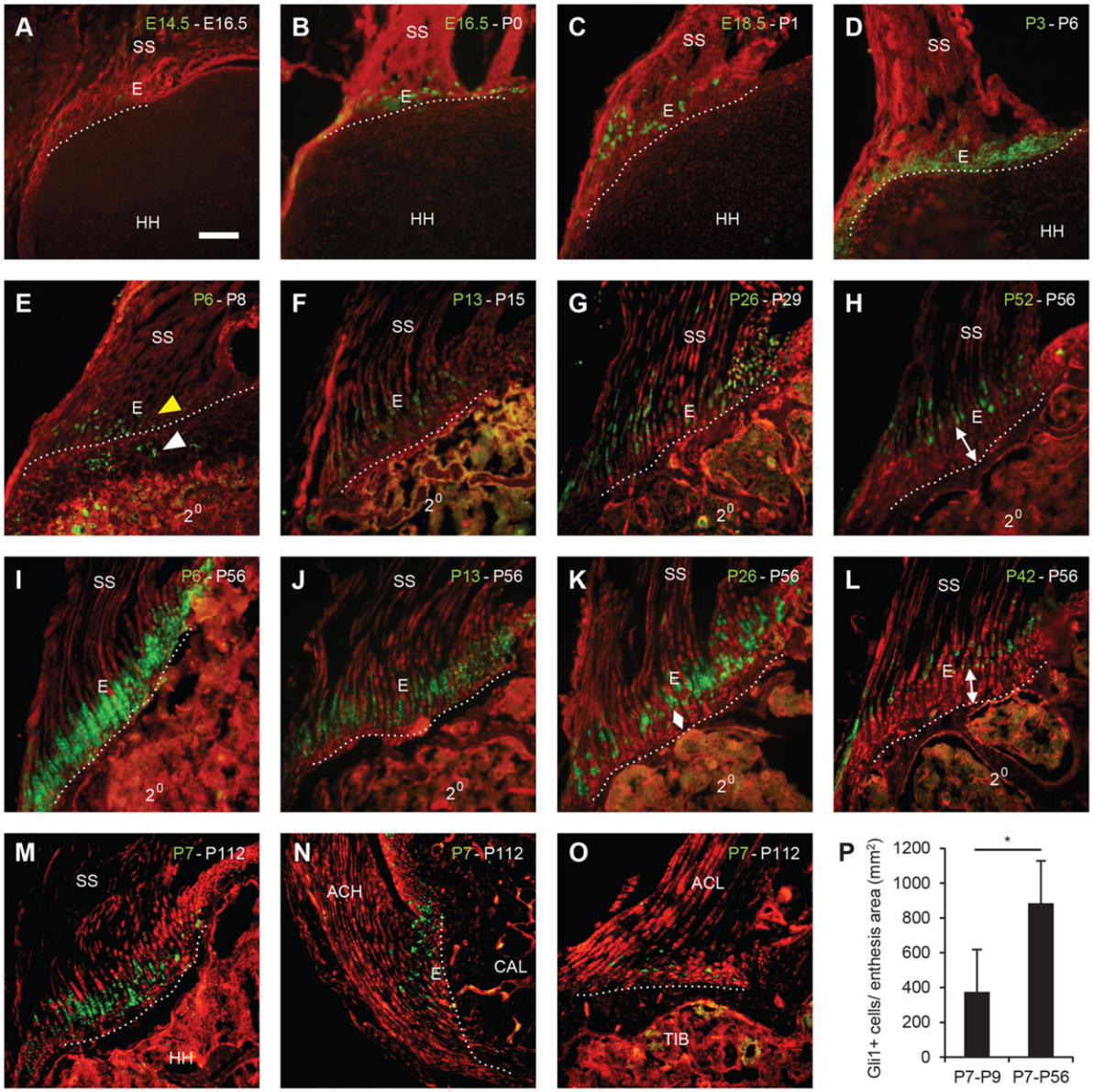

Fig. 1. The enthesis is derived from a unique population of Hh-responsive cells. *Gli1-Cre^{ERT2};mTmG* mice were labeled by Tamoxifen (TAM) injection on the day indicated in green and euthanized on the day indicated in white. (A-H) Hh-responsive cells are present in the enthesis throughout development. This cell population was initially located at the interface between the epiphyseal cartilage and the tendon (dotted lines). A second population of Hh-responsive cells was associated with the mineralization front of the secondary ossification center by P8 (E, white arrowhead), distinct from the population in the enthesis (E, yellow arrowhead). Once enthesis mineralization began (F-H), the Hh-responsive cell population shifted toward non-mineralized areas of the insertion. (I-O) Lineage-tracing experiments demonstrating that the Hh-responsive cell population identified during early postnatal development populated the mature insertion. Double-headed arrows (H,K,L) demonstrate that the Hh-responsive cell population shifted toward the unmineralized side of the insertion after P29. (P) The size of the Gli1-positive cell population increased significantly from P7 to P56 (N=5) (*P<0.05). SS, supraspinatus tendon; E, enthesis; HH, humeral head; ACH, Achilles tendon; CAL, calcaneus; ACL, anterior cruciate ligament; TIB, tibia; 2°, secondary ossification center. Scale bar: 100 µm.

observed in the enthesis in the early postnatal period. Labeling cells by TAM administration on P3 and EdU on P5 identified only a few proliferating cells (green) near the edges of the Hh-responsive cell population (red) (supplementary material Fig. S4A). Labeling cells with EdU on P14 and P42 (2 days post TAM administration) revealed no rapidly proliferating cells overlapping with the Hh-responsive cell population or any of the enthesis fibrocartilage cells (supplementary material Fig. S4B,C). By contrast, proliferating cells were observed in the proliferating zone of the adjacent growth plate (supplementary material Fig. S4D-F) and in the articular cartilage (supplementary material Fig. S4G). These results suggest that the Hh-responsive cell population that populates the enthesis proliferates more slowly than other types of chondrocytes.

Besides cell proliferation, tissue growth can occur by an increase in extracellular matrix volume accompanied by a decrease in cell density. To examine this possibility, we measured cell density as a function of animal age for the enthesis (supplementary material Fig. S4H). Cell density was defined as the total number of DAPI-stained nuclei at the enthesis per tissue area [i.e. the region marked by the Gli1 lineage tracing, including the cells within the mineralized fibrocartilage (MFC), which were not Hh responsive at the later postnatal time points]. Cell density at the enthesis decreased ~60% between birth and P42.

Development (2015) 142, 196-206 doi:10.1242/dev.112714

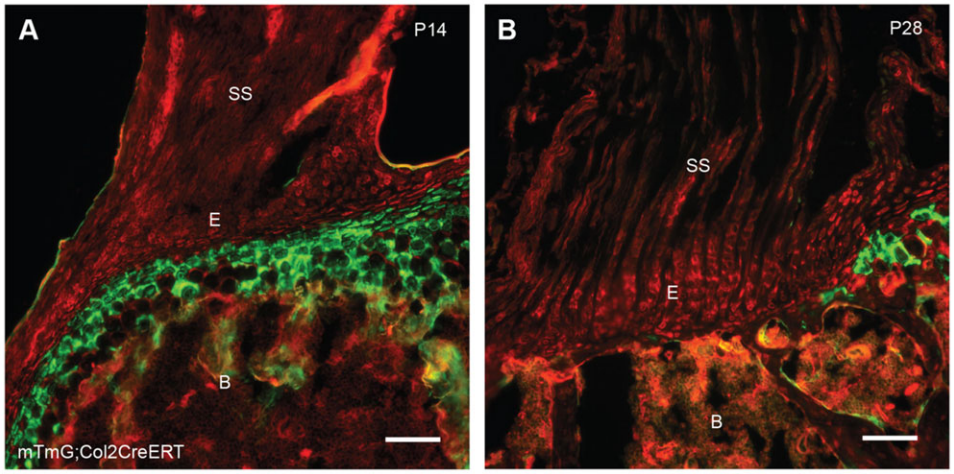

Fig. 2. *Col2-Cre^{ERT}* cells do not populate the developing tendon enthesis. *Col2-Cre^{ERT};mTmG* mice received injections of TAM twice per week until sacrifice on P14 (A) or P28 (B). *Col2*-positive cells within the epiphyseal cartilage display green fluorescence. SS, Supraspinatus tendon; B, bone; E, enthesis. Scale bars: 100 µm.

Reduced muscle loading increases the Hh-responsive cell population and Hh signaling at the enthesis

Since the Ihh-expressing chondrocytes in the growth plate are known to be modulated by mechanical loading (Nowlan et al., 2008; Wu et al., 2001), we next examined the effect of muscle forces on the population of Ihh-responsive cells in the enthesis during postnatal development. One limb of *Gli1-Cre^{ERT2};mTmG* animals was paralyzed by periodic injection with botulinum toxin A (BtxA) beginning on P1, and the contralateral limb received simultaneous saline injections (Schwartz et al., 2013). Hh-responsive cells, labeled by TAM administration 2-3 days prior to each time point, were measured by counting the number of Gli1-positive (green) cells compared with the total number of enthesis cells (DAPI stained) at each time point. The size of the Hh-responsive cell population was not affected by BtxA-induced mechanical unloading at P14 (Fig. 3A,D). However, at later time points (P28 through P56), paralyzed limbs had significantly increased numbers of Hh-responsive cells in the enthesis relative to controls (Fig. 3B versus E, and C versus F).

Gene expression analysis was then used to measure the relative expression level of genes involved in the Hh signaling pathway in paralyzed limbs compared with contralateral controls. RNA was extracted from laser micro-dissected regions of the enthesis encompassing both mineralized and non-mineralized fibrocartilage (a limitation of this method is the poor quality of the RNA yields; however, RNA quality did not differ between groups). Expression levels of *Smo* and *Ptch1* were not significantly affected by unloading at P7, but *Smo* expression was significantly upregulated at P21 and P42 in the BtxA-treated unloaded entheses relative to contralateral controls (Fig. 3H). *Ptch1* expression was significantly upregulated at P56 and showed a trend toward upregulation at P21 (P=0.07; Fig. 3I). Taken together, these results suggest that muscle forces are crucial at later stages of postnatal enthesis development to modulate Hh signaling and promote enthesis maturation.

Ablating the Hh-responsive cell population inhibits fibrocartilage development

To determine if the Hh-responsive cell population is required for fibrocartilage formation at the enthesis, *Gli1-Cre^{ERT2}* animals (Ahn and Joyner, 2004) were crossed with DTA mice (Voehringer et al., 2008). In these mice, Cre-expressing cells produce diphtheria toxin A (DTA), ablating the cell that produces it. The timing of cell ablation was controlled by TAM injection. Since this model would lead to ablation of all Hh-responsive cells throughout the body, we injected TAM at P6 to ablate enthesis cells (see Fig. 1D for an example of targeted cells) while minimizing damage to other developing organs. P6-injected *DTA;Gli1-Cre^{ERT2}* mice were viable past P42, although they were significantly smaller than TAM-injected littermate controls by P14 (Table 1). One limitation to this experiment is that fibrocartilage differentiation is likely to begin before P6 (e.g. supplementary material Fig. S1). Although mature fibrocartilage was not yet histologically evident at this time point, these animals had a much narrower zone of fibrocartilage (supplementary material Fig. S5). However, they did not completely lack fibrocartilage when the cell population was ablated.

Safranin-O staining of decalcified sections showed that cells populating the region of supraspinatus enthesis fibrocartilage lacked purple-stained nuclei by P14 through P42 (Fig. 4A-F). The absence of nuclei at P42 was further verified by a lack of DAPI staining (Fig. 4G,J). Additionally, the Safranin-O staining was less intense in *DTA;Gli1-Cre^{ERT2}* mice at P28 and P42 than in littermate controls (Fig. 4B,C,E,F, red stain). This indicates that the enthesis proteoglycan content was reduced in *DTA;Gli1-Cre^{ERT2}* mice. These results indicate that DTA expression in the Gli1 lineage cells effectively ablated the enthesis cells, supporting the idea that the Gli1 lineage cells are responsible for the formation and/or maintenance of the enthesis fibrocartilage.

We observed very little remodeling of the enthesis fibrocartilage even 5 weeks after cell ablation. No evidence of vascular invasion or matrix degradation was observed. These results are consistent with the observation that the Gli1 lineage cells in the enthesis do not rapidly proliferate (supplementary material Fig. S4).

Von Kossa staining suggested a decreased amount of MFC in *DTA;Gli1-Cre^{ERT2}* mice compared with littermate controls (Fig. 4H,K). These mice were smaller than littermate controls at P42 and had smaller, poorly mineralized humeral heads, indicative of aberrant overall mineralization (Table 1). Despite this, the average mineral density of the MFC was unchanged (Table 1). The volume of MFC was estimated using micro-computed tomography (microCT) and normalized to the humeral head volume to scale for the overall size and mineralization defects observed in these mice (an example microCT image is shown in Fig. 4L). The normalized MFC volume was significantly reduced in *DTA;Gli1-Cre^{ERT2}* animals compared with littermate controls (Fig. 4I). This indicates that the mineralization defect in the enthesis was more severe than that in the underlying bone.

Development (2015) 142, 196-206 doi:10.1242/dev.112714

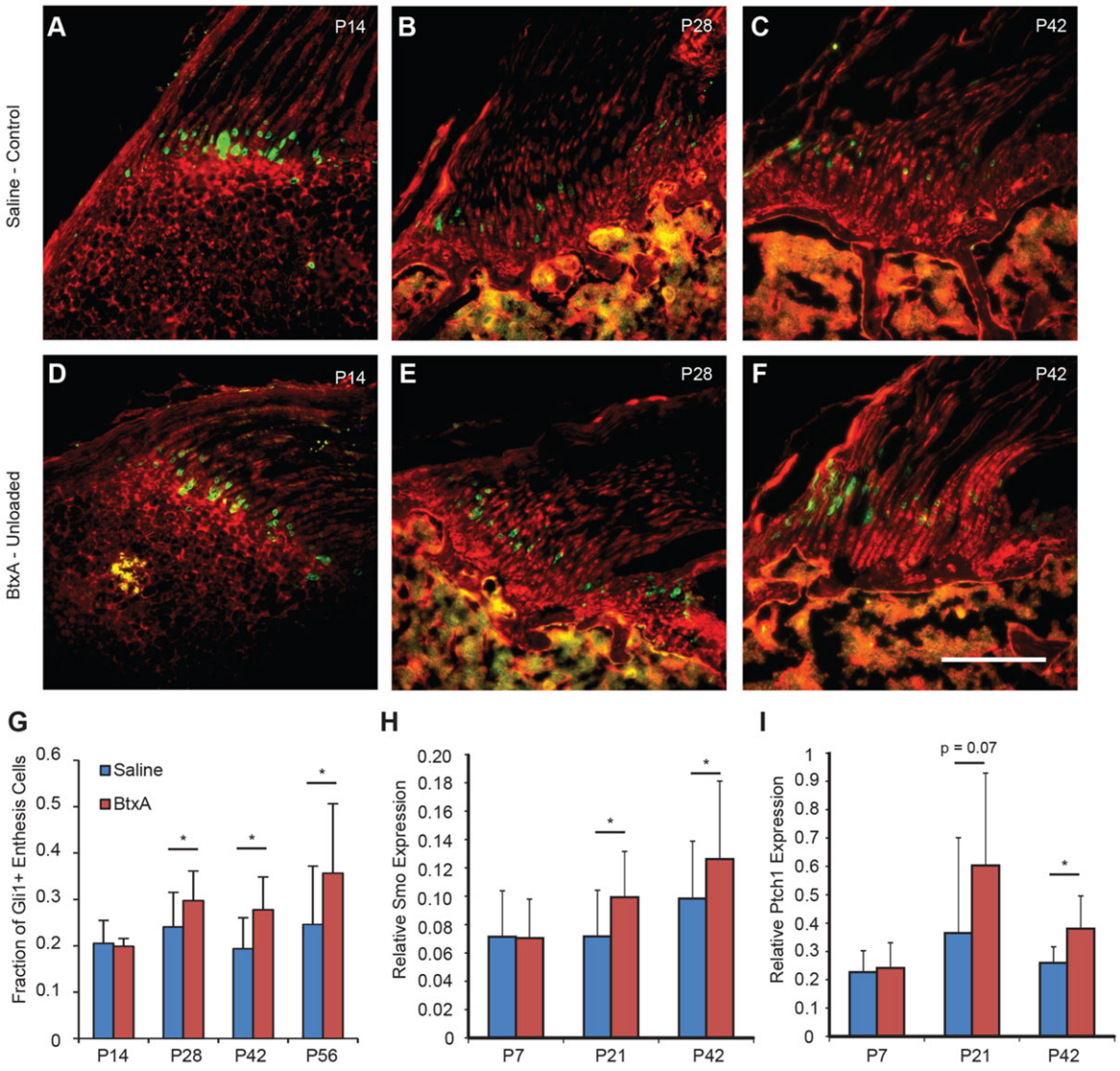

Fig. 3. BtxA-induced paralyses lead to increases in the Hh-responsive cell population in the postnatal enthesis. Supraspinatus entheses from paired control *Gli1-Cre^{ERT2};mTmG* shoulders (A-C) and paralyzed shoulders (D-F) are shown. Animals were injected with TAM 2-3 days prior to sacrifice on P14 (A,D), P28 (B,E) or P42 (C,F) to label the Hh-responsive cell population (green cells). (G) Quantification showed that the Hh-responsive cell population was increased by BtxA-induced mechanical unloading (*N*=4-5). (H,I) RT-qPCR gene expression analysis of BtxA unloaded and control shoulders supported this finding. Expression of *Smo* (H) and *Ptch1* (I) was increased relative to *Gapdh* during late postnatal development (*N*=4-5). **P*<0.05. Scale bar: 200 µm.

Reduced Ihh signaling decreases fibrocartilage mineralization

To investigate the necessity of Hh signaling for enthesis development, *Smo$^{fl/fl}$* mice (Long et al., 2001) were crossed with *ScxCre* mice (Blitz et al., 2009). Deletion of Smo, a molecule necessary for Hh signaling, was targeted to tendon and enthesis progenitor cells using the *ScxCre* mouse model. Recent studies identified a fetal progenitor population of cells positive for both Scx and Sox9 at the junction of developing tendon and as-yet unmineralized bone (Blitz et al., 2013; Sugimoto et al., 2013). Using a reporter mouse, we verified that ScxCre targeted all of the enthesis and tendon cells (supplementary material Fig. S6). There was a severe mineralization defect in the MFC of *ScxCre;Smo$^{fl/fl}$* (cKO) mice at P56. Staining the mineral using von Kossa's method showed that entheses from cKO animals at P56 had severely disrupted mineralization relative to controls (Fig. 5A,B). Histomorphometric analysis of fibrocartilage thickness revealed that the zone of MFC was thinner in cKO animals while the zone of non-MFC was thicker (Fig. 5C). The overall thickness of the entire fibrocartilage was not significantly different between the two groups. This suggests that deletion of Smo caused a defect in mineralization of the fibrocartilage that is likely to have resulted from changes in the phenotype of the fibrocartilage cells. In support of this, Toluidine Blue staining of decalcified sections showed a wider region of non-mineralized fibrocartilage, with large round fibrochondrocytes (Fig. 5D,E). These cells were less numerous (Fig. 5F) and significantly larger than fibrochondrocytes from control animals (cell diameter of 8.9±0.6 µm versus 7.2±0.3 µm), suggesting defects in proliferation and differentiation. This is consistent with previous results demonstrating that Ihh regulates the transition from round, resting/early proliferative chondrocytes to stacked columnar chondrocytes in the growth plate (Hilton et al., 2007; Kobayashi et al., 2005).

MicroCT analysis revealed that both the MFC volume and mineral density were significantly reduced in cKO mice compared with littermate controls (*Smo$^{fl/fl}$*) (Fig. 5G,H). By contrast, no

Development (2015) 142, 196-206 doi:10.1242/dev.112714

Table 1. MicroCT analysis of P42 *DTA;Gli1-Cre^{ERT2}* mice

			Humeral head			
Group	Body weight (g)	Insertion BMD (mg HA/cm^3)	TV (cm^3)	BV (cm^3)	BV/TV	BMD (mg HA/cm^3)
DTA;Gli1-Cre	10.43 (2.08)*	569.23 (32.63)	3.52 (0.55)*	2.21 (0.41)*	0.63 (0.02)*	308.08 (16.44)‡
Control	17.38 (1.45)	573.54 (24.79)	4.37 (0.27)	3.02 (0.23)	0.69 (0.04)	345.47 (29.12)

Mean values are shown with s.d. in parentheses. BMD, bone mineral density; BV, bone volume; HA, hydroxyapatite; TV, total volume.
*P<0.05, ‡P=0.057, relative to control.

differences were observed in trabecular bone parameters within the humeral head, suggesting that the mineralization defect was localized to the entheses (Table 2). This result is consistent with the expression pattern of ScxCre, which targets fibrocartilagenous attachments but not the remainder of the epiphysis. Synchrotron-based X-ray diffraction (XRD) analysis of the MFC indicated that the size of the hydroxyapatite crystals was reduced in cKO animals compared with controls (Fig. 5I). The coefficient of variation of the crystal grain sizes among the 20 analysis spots within each sample was narrower in cKO animals than in controls (Table 2). No significant differences in the mineral crystal orientation (FWHM of azimuthal intensity) or mineral ε_{RMS} were observed (Table 2).

Uniaxial tensile testing was used to evaluate the biomechanical changes caused by loss of Hh signaling in the enthesis during

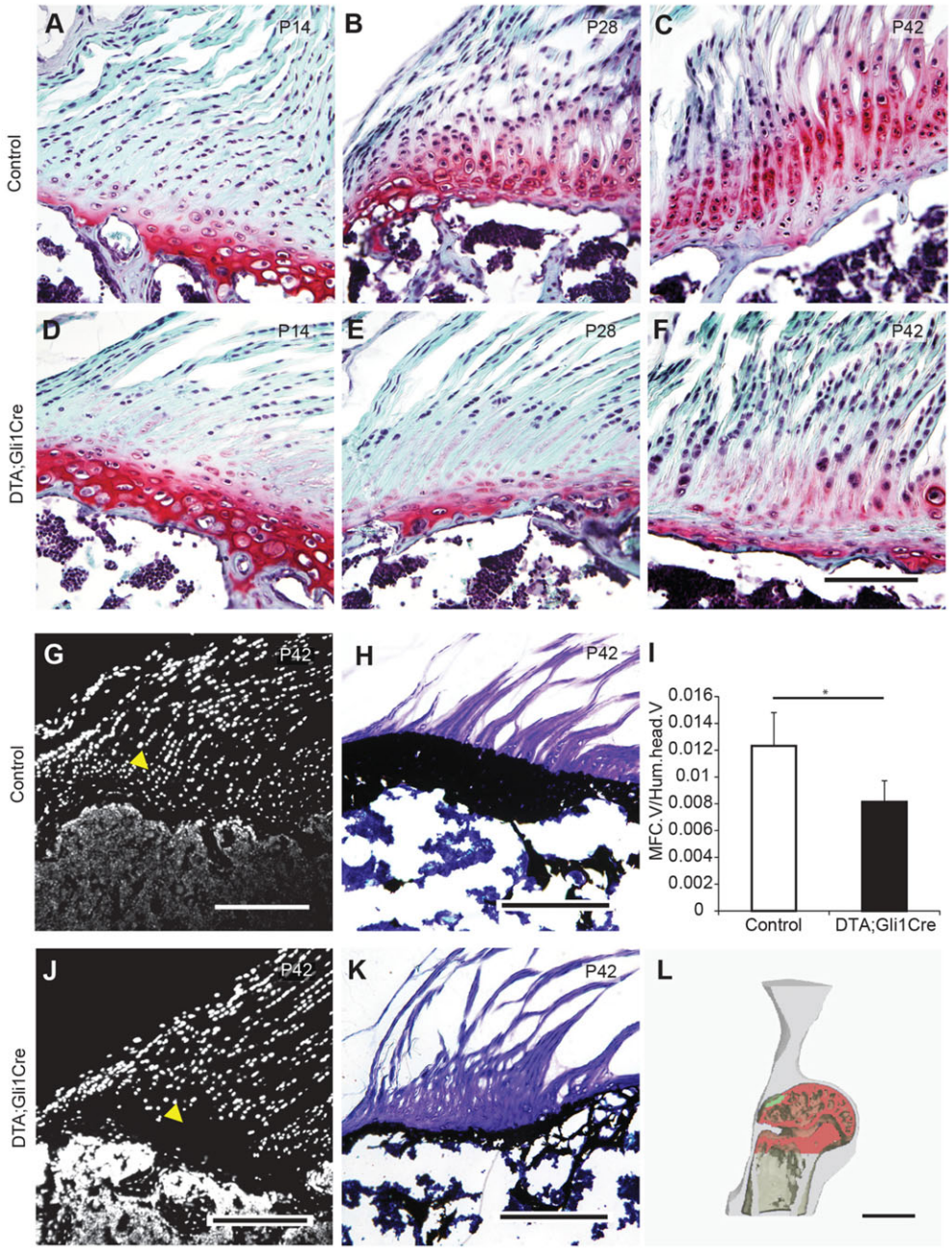

Fig. 4. Ablation of the Hh-responsive cell population results in a loss of enthesis fibrocartilage. (A-F) Safranin-O staining indicated a loss of enthesis proteoglycan in ablated entheses relative to controls. (G,J) DAPI-stained 6 week control and *DTA;Gli1-Cre^{ERT2}* sections demonstrated a loss of nuclei (yellow arrowhead) in the enthesis that was not recovered 5 weeks post cell ablation. (H,K) Von Kossa staining suggested a decrease in mineralized fibrocartilage (MFC) in *DTA;Gli1-Cre^{ERT2}* compared with control (note that there is an artifactual tear in the center of the histologic section shown in K). (I) MicroCT analysis demonstrated that MFC volume relative to the humeral head volume was decreased in *DTA;Gli1-Cre^{ERT2}* compared with control (N=4-5) (*P<0.05). (L) An example of MFC volume (green area) relative to the humeral head volume (red area) from a control animal. Scale bars: 100 µm in A-F; 200 µm in G,H,J,K; 1 mm in L.

Development (2015) 142, 196-206 doi:10.1242/dev.112714

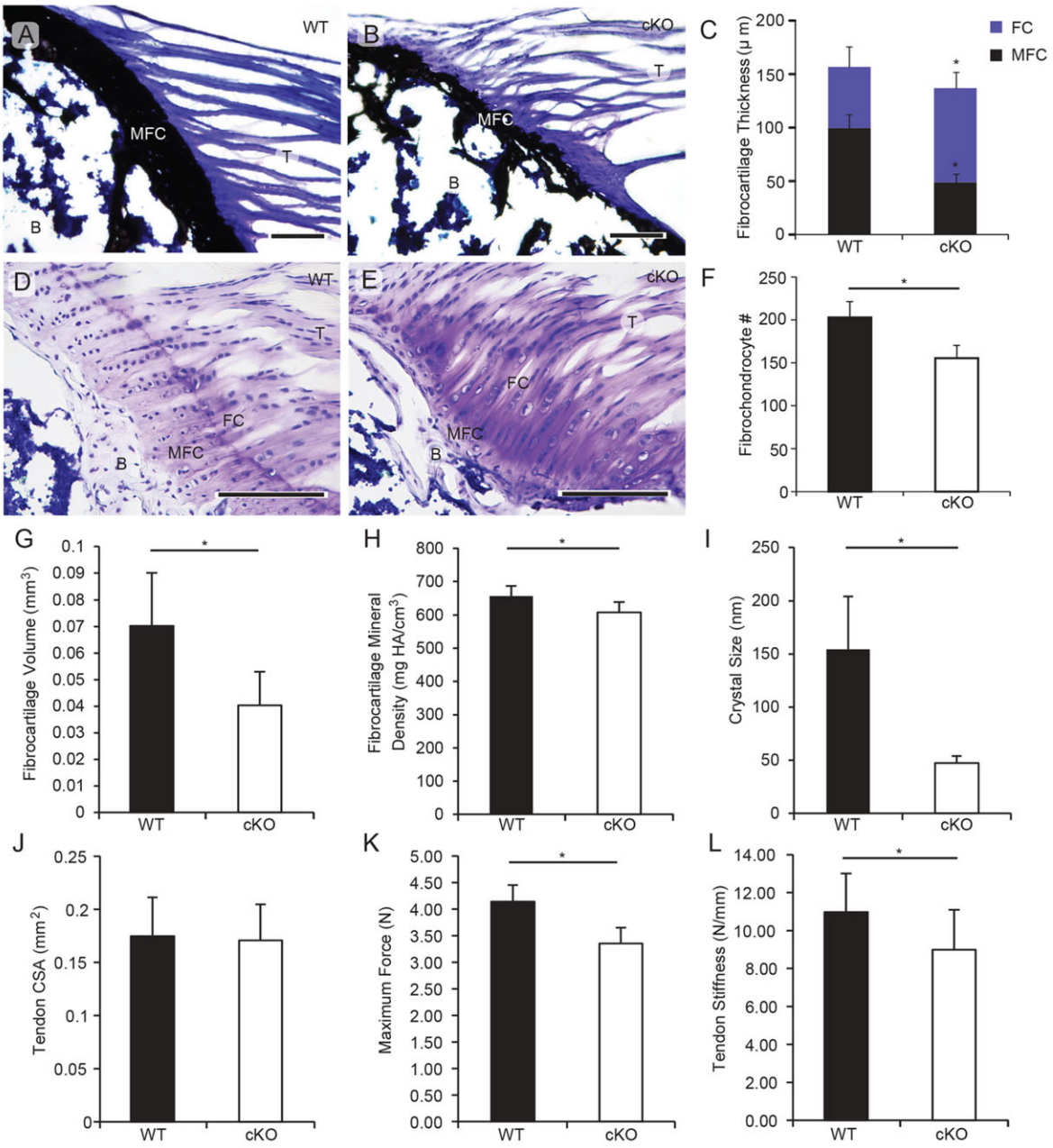

Fig. 5. Hh signaling is necessary for enthesis fibrocartilage mineralization. (A,B) Von Kossa staining in control and *ScxCre;Smo*$^{fl/fl}$ (cKO) entheses demonstrated aberrant mineralization in cKO animals. (C) Fibrocartilage thickness was increased and MFC was decreased in cKO entheses compared with control entheses (*N*=5). (D,E) Toluidine Blue staining suggests disrupted fibrocartilage differentiation and proliferation. (F) Fibrocartilage cell number is reduced in cKO animals compared with controls. T, tendon; FC, fibrocartilage; MFC, mineralized fibrocartilage; B, bone. Scale bars: 100 μm. (G,H) MicroCT quantification of MFC volume and mineral density demonstrated a mineralization defect in cKO compared with control mice (*N*=12). (I) Hydroxylapatite crystal size, as measured by XRD, was reduced in cKO compared with control mice (*N*=3). (J) Tendon cross-sectional area was unchanged in cKO compared with control mice (*N*=12). (K,L) Uniaxial tensile testing revealed that enthesis function was impaired in cKO compared with control mice. Specifically, the ultimate strength and stiffness of the supraspinatus enthesis were reduced (*N*=12). **P*<0.05.

development. The tendon cross-sectional area was not significantly altered in the cKO mice (Fig. 5J). Tendon enthesis strength and stiffness, however, were significantly reduced in these animals compared with controls (Fig. 5K,L). Additionally, the normalized biomechanical properties of maximum stress, yield stress, yield strain, and the energy to yield (modulus of resilience) were significantly reduced in cKO animals compared with controls (Table 3). Together, these results indicate that removing Hh signaling in tendon and enthesis progenitors throughout development results in reduced mechanical properties of the enthesis.

DISCUSSION

A unique population of Gli1-positive cells exists at the enthesis in the perinatal period that is distinct from tenocytes and epiphyseal chondrocytes. This cell population appears well before the onset of mineralization at the enthesis and persists in the mature enthesis. Lineage-tracing experiments demonstrated that these cells and their progenies remain at the enthesis throughout postnatal development and populate the entire region of fibrocartilage between tendon and bone (Fig. 6). This suggests that Gli1 might be a marker for a population of enthesis progenitor cells. Additionally, Gli1 has been

Development (2015) 142, 196-206 doi:10.1242/dev.112714

Table 2. Mineralization patterns in *ScxCre;Smo$^{fl/fl}$* (cKO) versus *Smo$^{fl/fl}$* (control) mice

	Humeral head microCT analysis (*N*=12)							MFC XRD (*N*=3)		
Group	BV/TV	Conn-Dens.	BMD	Tb.N	Tb.Th	Tb.Sp	Humeral length	FWHM	εRMS	Crystal Size Cov.
cKO	0.32 (0.09)	140 (28)	338 (46)	6.19 (0.87)	0.07 (0.01)	0.16 (0.03)	11.05 (0.40)*	68.0 (5.22)	80,702 (16,781)	0.26 (0.05)*
Control	0.32 (0.07)	135 (23)	334 (34)	6.14 (0.40)	0.07 (0.01)	0.16 (0.02)	11.66 (0.30)	60.0 (5.22)	72,967 (5542)	0.41 (0.05)

MicroCT analysis indicated no differences in trabecular architecture in cKO animals. Average values are shown with s.d. in parentheses. MFC, mineralized fibrocartilage; XRD, X-ray diffraction; BV, bone volume; TV, total volume; BMD, bone mineral density; Conn-Den, connectivity density; Tb.N, trabecular number; Tb.Th, trabecular thickness; Tb.Sp, trabecular spacing; FWHM, full width half maximum; εRMS, root mean square strain; Cov., covariance.
*P<0.05, relative to control.

shown to be a marker of progenitor cells in mature organisms and a small population of Gli1-positive cells persists in the mature enthesis at the edge of the mineralization front (Brownell et al., 2011; Seidel et al., 2010; Zhao et al., 2014). This cell population is likely to contribute to the advancement of the mineralization front and widening of the enthesis as the animal grows.

The development and growth processes in the enthesis driven by this cell population are similar to endochondral bone formation, with one major distinction: this region is never remodeled into bone. Rather than being vascularized and replaced by osteoclasts and osteoblasts, enthesis chondrocytes in the MFC stop expressing Gli1 and remain viable. This model of enthesis formation is supported by our results using *DTA;Gli1-Cre^{ERT2}* mice; the fibrocartilage in these mice remained acellular and the matrix was not remodeled 5 weeks after cell ablation. This tissue is therefore likely to lack the pro-angiogenic and matrix degradation signals necessary to promote tissue remodeling. It is also a likely factor in the poor healing response seen at adult tendon-to-bone interfaces (Kovacevic and Rodeo, 2008; Silva et al., 2006; Thomopoulos et al., 2002).

Although the *DTA;Gli1-Cre^{ERT2}* model demonstrated the necessity of the Gli1-positive cell population for the development of enthesis fibrocartilage, the role of Hh signaling itself remains less clear. Removing Hh signaling from enthesis cells using the *ScxCre;Smo$^{fl/fl}$* model affected enthesis chondrocyte proliferation and differentiation. These results are consistent with earlier reports describing the role of Hh in perichondrial development (Hojo et al., 2013; Long et al., 2004, 2001). The enthesis fibrocartilage cells might also originate from this cell population, but differentiate later in development than other structures of the developing bone, with fibrocartilage becoming histologically evident at the enthesis at ∼P7-P14. In the Hh signaling-deficient cKO animals, despite a reduced number of cells, a region of fibrocartilage persisted in the enthesis that was comparatively less mineralized than in controls. Reducing Hh signaling specifically in enthesis and tendon progenitor cells did not result in loss of the fibrocartilage cell lineage. This suggests that, although Hh signaling is likely to be required for the postnatal differentiation of this cell population that leads to MFC formation, the role of activated Hh signaling in the late embryonic enthesis remains unclear.

Our results further suggest that the postnatal fibrocartilage differentiation process might be modulated by the loading environment. When muscle loading was removed at birth, there was an increase in the number of Hh-responsive cells at P28. This result complements previous studies that have shown that Ihh expression is either upregulated or downregulated in response to increased or decreased cyclic compressive loading, respectively (Chen et al., 2009; Ng et al., 2006; Shao et al., 2012; Wu et al., 2001). In the current study, decreased cyclic tensile loads led to increased Ihh signaling. This was accompanied by a mineralization defect in the humeral head and increased osteoclast activity, which suggests increased resorption and remodeling of the endosteal surface of the MFC (Thomopoulos et al., 2007). These results support the idea that decreased Hh signaling in the MFC might be related to cellular changes in the fibrocartilage that lead to stable MFC and prevent its remodeling into bone. The unloading experiments in the current study demonstrate that muscle forces play a key role in reducing Gli1 expression in MFC after mineralization, possibly preventing tissue degradation and remodeling into bone.

Hh signaling also plays an important role during the earliest stages of postnatal enthesis development. Mineralization of the enthesis occurs between P7 and P14; the cell ablation experiments, performed within this time frame, demonstrated that the Hh-responsive cell population is crucial for normal mineralization. Mineralization during this time period might be driven by biochemical signals and less influenced by muscle loads, as evidenced by there being no changes in gene expression due to unloading at P7. This is consistent with the findings of Blitz et al. (2009), who showed that the initiation of bone ridge formation required only biochemical signals from the tendon, whereas the subsequent growth phase required muscle forces. Furthermore, removal of Hh signaling in cells from tendon-specific and enthesis-specific lineages led to severely disrupted fibrocartilage development. This process might be modulated by another pathway, such as BMP signaling. Blitz et al. (2009) showed that Scx expression in tendon cells regulates Bmp4, leading to bone ridge formation at tendon attachment sites. BMP signaling has also been shown to induce Ihh signaling in chondrocytes (Grimsrud et al., 2001; Minina et al., 2001). Based on these findings, it is probable that BMP signaling drives enthesis chondrocyte differentiation, whereas Hh signaling is subsequently required for enthesis mineralization.

In contrast to the substantial mineralization defect observed in the enthesis of the cKO mice, no mineralization defect was observed in the trabecular bone of the humeral head. This implies that the loss of fibrocartilage volume is not due to decreased thickness of the layer of trabecular bone underlying the MFC. We did observe a small but significant decrease in humeral length in these mice. This phenotype

Table 3. Biomechanical properties of *ScxCre;Smo$^{fl/fl}$* (cKO) versus *Smo$^{fl/fl}$* (control) mice

Group	Maximum stress (MPa)	Young's modulus (MPa)	Toughness (MPa)	Strain at max. stress	Strain at yield	Yield stress (MPa)	Modulus of resilience (MPa)
cKO	21.36 (5.35)*	105.29 (43.59)	6.22 (2.42)	0.34 (0.13)	0.29 (0.11)*	18.31 (4.78)*	2.75 (1.68)*
Control	26.24 (5.81)	121.89 (44.18)	7.50 (2.43)	0.43 (0.10)	0.39 (0.11)	23.15 (6.32)	4.63 (2.10)

Mean values are shown with s.d. in parentheses. *P<0.05, relative to control.

Development (2015) 142, 196-206 doi:10.1242/dev.112714

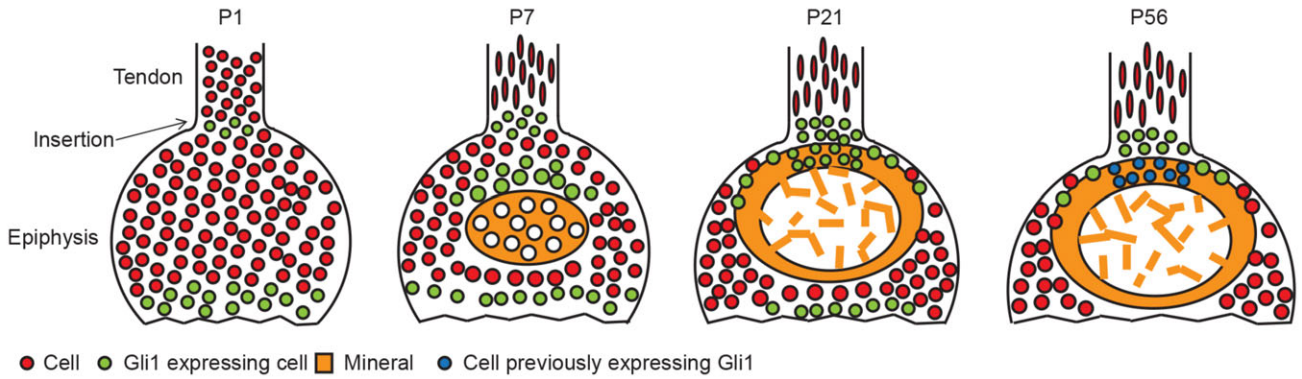

Fig. 6. Development of the enthesis, showing cell populations in which Hh is active. In neonatal mice, Hh-responsive cells (green) are present at the tendon-epiphyseal cartilage interface and the primary growth plate before the secondary ossification center appears. Once the secondary ossification center is established ~1 week after birth (orange), an additional Hh-responsive cell population is observed at the mineralization front that is distinct from the population at the tendon interface. The Hh-responsive hypertrophic cells associated with the mineralization front are remodeled into bone by 3 weeks after birth, while the Hh-responsive cells at the tendon interface populate the mineralizing enthesis fibrocartilage. By late postnatal development, these cells remain alive in the MFC but are no longer Hh responsive (blue). The Hh-responsive cell population shifts toward the non-mineralized FC.

might be caused by the *ScxCre* model targeting the cell populations that lead to the bony prominences at the ends of bones, which contribute to overall bone length (Blitz et al., 2013; Sugimoto et al., 2013). These prominences are often attachment sites for tendons and ligaments. Lending further support to defective fibrocartilage mineralization in this model, we observed that the size of the mineral crystals is reduced, as well as their size distribution. This is consistent with a less mature mineralized matrix in which hydroxyapatite has perhaps been more recently deposited on the collagen template (e.g. nucleation has occurred on the collagen template but crystal growth has been limited) (Legros et al., 1987; Miller et al., 2001). The reduced biomechanical function of the enthesis suggests that the zone of MFC is crucial for modulating the transfer of muscle loads from tendon to bone.

The source of the Hh ligand during enthesis development and maturation remains unclear. Ihh is a likely candidate because it is known to act in a paracrine fashion during endochondral bone development. The sources of the Ihh ligand in this case are the pre-hypertrophic and early hypertrophic cells in the primary ossification center (Long et al., 2001; Vortkamp et al., 1996, 1998) (supplementary material Fig. S3A). The cells that respond to Ihh are found in the perichondrium and the growth plate proliferating zone. As the enthesis cells are in close proximity to these cell populations, Ihh might also be responsible for Gli1 expression in the enthesis. Although Liu et al. (2013) showed by immunofluorescence that Ihh, and not sonic hedgehog, was expressed in the neonatal patellar tendon enthesis, we cannot definitively rule out the possible involvement of other Hh ligands from different cell sources.

In summary, a unique population of cells was identified in the fibrocartilagenous enthesis that were Gli1 positive in the perinatal period and eventually fully populated the mature enthesis fibrocartilage. Later during postnatal life, the size of the Hh-responsive population was influenced by muscle loading. Ablation of this population resulted in a cell-free enthesis weeks after cell death, suggesting that this tissue is resistant to remodeling and that a loss of this fibrocartilage cell population due to injury is likely to be permanently detrimental to the enthesis. Removal of Hh signaling in these cells affected the postnatal phenotype of enthesis chondrocytes, leading to defects in fibrocartilage mineralization. These results suggest that this cell population and Hh signaling may play a crucial role in fibrocartilage healing after injury.

MATERIALS AND METHODS

Animal models

The use of animals for this study was approved by the Animal Studies Committee at Washington University. Male and female animals were used in equal proportion. For lineage-tracing experiments, TAM-inducible *Gli1-Cre^{ERT2}* mice (Ahn and Joyner, 2004) were crossed with *Rosa26-mTmG* (*mTmG*) mice (Jackson Laboratory). TAM was dissolved in corn oil and 100-200 µg/g body weight was injected subcutaneously between the shoulder blades at the time points indicated. At least three animals were used for each labeling experiment. For comparison, *Col2-Cre™;mT/mG* mice were also used (Hilton et al., 2007). For cell ablation experiments, *Rosa-DTA* (*DTA*) mice were crossed with *Gli1-Cre^{ERT2}* animals (Voehringer et al., 2008). These animals received 200 µg/g body weight TAM on P6 (N=5 per time point). *ScxCre* mice (Blitz et al., 2009) were crossed with *Smo$^{fl/fl}$* (Long et al., 2001) mice to investigate the conditional knockdown of Ihh signaling at P56.

Histology/histomorphometry

Following euthanasia, the humerus, supraspinatus tendon and muscle were dissected free of all other tissues, fixed in 4% paraformaldehyde (PFA), decalcified with 14% EDTA, embedded in OCT medium (Sakura Finetek), and sectioned on a cryostat. Sections for fluorescence imaging were washed with PBS and mounted with aqueous mounting medium (Fluoromount, Electron Microscopy Sciences). Sections used for cell counting were mounted with aqueous medium containing DAPI. Additional sections were stained with Safranin-O and Toluidine Blue. Mineralized frozen sections were cut using Cryofilm (Section Lab) and stained by von Kossa's method followed by Toluidine Blue.

Cell number and cell size were measured using ImageJ software (Schneider et al., 2012). A polygon was drawn to measure the area of the enthesis encompassing the zone of fibrocartilage on each slide and cells within this area were counted or measured. Counting was performed on two sections per animal and regions with large histological artifacts were excluded from analysis.

In situ hybridization

In situ hybridization was performed on frozen tissue sections using a ^{35}S-labeled riboprobe for *Ihh* as previously described (Long et al., 2001).

Botulinum toxin unloading model

BtxA was injected according to published protocols (Schwartz et al., 2013; Thomopoulos et al., 2007). Briefly, *Gli1-Cre^{ERT2};mTmG* animals were injected with 0.2 U in 10 µl sterile saline starting at P1, twice per week, until sacrifice, and the contralateral limb was injected concurrently with the same volume of saline (four or five animals were used for each time point of each assay). These animals also received injections of TAM 2-3 days prior to sacrifice to label cells in which Hh is active.

Development (2015) 142, 196-206 doi:10.1242/dev.112714

Laser capture micro-dissection and RT-qPCR

The murine enthesis has cellular, structural and compositional properties that are distinct from the adjacent tendon and bone. Laser capture micro-dissection was therefore used to isolate cells from this tissue to study localized gene expression levels within the enthesis fibrocartilage without contamination from the adjacent tendon and bone. Freshly dissected humerus-supraspinatus tendon complexes were frozen in OCT medium under RNase-free conditions using dry ice. Sections were cut at 30 µm using laser capture microscopy (LCM) tape (Section Lab) on a cryostat. The tape sections were then mounted on plastic slides containing a hole for laser capture micro-dissection using an LMD7000 system (Leica Microsystems). Sections were briefly thawed, then micro-dissected and deposited into caps filled with lysis buffer. The Norgen Total RNA Micro Kit (Thorold) with additional proteinase K digestion and DNase I treatment was used to extract RNA. Each RNA sample was converted to cDNA using the Superscript VILO cDNA Synthesis Kit (Life Technologies). RNA was quantified using the Agilent RNA 6000 Pico Kit with the Agilent Bioanalyzer. As is typical for LCM experiments, RNA yields were relatively low (0.2-1 ng/µl), with low RNA integrity numbers (1.5-3). However, there were no significant differences between groups for RNA yield or integrity, so the overall trends in the data are likely to be representative. Real-time PCR was performed using TaqMan chemistry on a StepOnePlus Real-Time PCR System (Applied Biosystems). Primers for *Smo* (Mm01162710_m1), *Ptch* (Mm00436026_m1) and glyceraldehyde 3-phosphate dehydrogenase (*Gapdh*) (Mm99999915_g1) were purchased from Life Technologies. PCR reactions were performed in duplicate and a third reaction was performed for samples where the first two reactions were inconsistent. All results are expressed as fold change relative to the housekeeping gene *Gapdh*.

Micro-computed tomography analysis

microCT (µCT40; Scanco Medical) was used to determine the volume of MFC, humeral head volume, humeral head trabecular architecture, and tendon cross-sectional area. Supraspinatus muscle-tendon-bone samples were fixed in 4% PFA prior to scanning. The distal humerus was potted in agarose in a plastic tube that was inverted within the sample holder. This suspended the supraspinatus tendon and muscle in air to optimize soft tissue contrast. Scans were performed at X-ray tube settings of 45 kV and 177 µA with a 200 ms integration time, resulting in a 20 µm voxel size.

The humeral head volume was estimated from all of the slices proximal to the distal end of the anatomic neck of the humerus. Trabecular architecture was measured from all slices proximal to the epiphyseal plate. Fibrocartilage volume was measured by manually drawing regions of interest around the dense mineralized areas adjacent to the supraspinatus tendon. Tendon cross-sectional area was determined from the axial slice with the minimum tendon area.

X-ray diffraction measurements

XRD experiments were performed at the Argonne National Laboratory using beamline 2I-D-D. Details are provided in the methods in the supplementary material. Briefly, frozen tissue sections from *ScxCre;Smo*$^{fl/fl}$ animals and littermate controls (N=3 per group) were mounted on silicon nitride windows (Silson) that were positioned normal to the incident X-ray beam. Following preliminary optical mapping, 20 spots were analyzed within the fully mineralized MFC region arranged in two rows of ten parallel to the mineral interface and spaced by 1 µm. The acquired diffraction patterns for each region of interest were analyzed using custom software (Deymier-Black et al., 2013). The diffraction rings were fitted and measures of crystallite size, angular intensity, crystal strain, and root mean square strain (ε_{RMS}) were averaged over the 20 mapped spots for each specimen.

Biomechanical testing

Supraspinatus tendons from 12 *ScxCre;Smo*$^{fl/fl}$ animals per group (cKO and control) were tested according to our previously published methods (Schwartz et al., 2013). Limbs were dissected to isolate the supraspinatus tendon, muscle and humerus and scanned with microCT to determine tendon cross-sectional area. The cross-sectional area was defined as the minimum tendon area determined from the series of axial slices spanning the tendon. Next, the humerus was potted in 1 Minute Epoxy (McMaster Carr) with an embedded paperclip to secure the proximal growth plate. The tendon was secured between single layers of paper using cyanoacrylate and then mounted in custom grips in a 37°C saline bath on an Instron Electropuls E1000 (Instron) fitted with a 5 N load cell. The gauge length was determined optically via a calibration standard on the top grip and was ~2 mm for all specimens. Tendons were subjected to five cycles of preconditioning (3% strain) before loading to failure in uniaxial tension at 0.5% strain/s (WaveMatrix software, Instron). Samples that failed either at the grip or the growth plate were excluded from all analyses.

The stiffness and ultimate force were defined as the slope of the linear region and maximum value, respectively, of the load-displacement curve. Load was normalized by the cross-sectional area and displacement was normalized by the initial tendon length to obtain stress-strain curves. The modulus, yield strength/stress, yield strain, resilience and toughness were then determined from the stress-strain curves. The ultimate stress was defined as the maximum value of the stress-strain curve. The toughness was defined as the total area under the stress-strain curve. Although all samples failed at the insertion of tendon into bone, this measure was highly variable due to the inconsistent post-failure behavior of the samples. The yield stress was therefore defined as the stress value when the tangent modulus decreased to 50% of the maximum value in the load-to-failure tests. The yield strain and energy to yield (i.e. modulus of resilience) were defined as the strain value and total area, respectively, under the stress-strain plot up to the yield stress.

Statistical methods

For the BtxA unloading model, BtxA-treated shoulders were compared with contralateral saline-treated shoulders using a paired t-test (N=5-6 per group). *DTA;Gli1-Cre*^{ERT2} animals were compared with age-matched littermate controls using ANOVA. *ScxCre;Smo*$^{fl/fl}$ animals were compared with littermate controls using an ANCOVA analysis to account for the effects of genotype and animal age using gender as a covariate in the analysis. Six males and six females of each genotype were tested mechanically and analyzed for microCT. Five animals per group were used for histomorphometric analysis. Significance was defined as P<0.05 and all data are reported as mean±s.d.

Acknowledgements

We thank Drs Alix Black, Zhonghou Cai and Jon Almer for assistance with the X-ray diffraction/fluorescence experiments performed at the Advanced Photon Source (APS) at the Argonne National Laboratory. XRD data were analyzed using software previously developed by Dr Jon Almer and modified by Dr Alix Deymier-Black for this application. We thank Crystal Idleburg for performing the cryosectioning for LCM; Jianquan Chen and Yu Shi for assistance with the *in situ* hybridization experiment; and Ronen Schweitzer for generously providing the *ScxCre* animals used in this study.

Competing interests

The authors declare no competing financial interests.

Author contributions

A.G.S., F.L. and S.T. designed the experiments and edited the manuscript. A.G.S. performed the experiments and analyzed the data.

Funding

This study was supported by the National Institutes of Health [R01 AR055580 to S.T., T32 AR060719 to A.G.S., R01 DK065789 to F.L. and P30 AR057237]. Use of the APS Sector 2I-D-D was supported by the US Department of Energy, Department of Science under contract DE-AC02-06CH11357. Deposited in PMC for release after 12 months.

Supplementary material

Supplementary material available online at
http://dev.biologists.org/lookup/suppl/doi:10.1242/dev.112714/-/DC1

References

Ahn, S. and Joyner, A. L. (2004). Dynamic changes in the response of cells to positive hedgehog signaling during mouse limb patterning. *Cell* **118**, 505-516.

Benjamin, M., Kumai, T., Milz, S., Boszczyk, B. M., Boszczyk, A. A. and Ralphs, J. R. (2002). The skeletal attachment of tendons–tendon "entheses". *Comp. Biochem. Physiol. A Mol. Integr. Physiol.* **133**, 931-945.

Blitz, E., Viukov, S., Sharir, A., Shwartz, Y., Galloway, J. L., Pryce, B. A., Johnson, R. L., Tabin, C. J., Schweitzer, R. and Zelzer, E. (2009). Bone ridge

patterning during musculoskeletal assembly is mediated through SCX regulation of Bmp4 at the tendon-skeleton junction. *Dev. Cell* **17**, 861-873.
Blitz, E., Sharir, A., Akiyama, H. and Zelzer, E. (2013). Tendon-bone attachment unit is formed modularly by a distinct pool of Scx- and Sox9-positive progenitors. *Development* **140**, 2680-2690.
Brownell, I., Guevara, E., Bai, C. B., Loomis, C. A. and Joyner, A. L. (2011). Nerve-derived sonic hedgehog defines a niche for hair follicle stem cells capable of becoming epidermal stem cells. *Cell Stem Cell* **8**, 552-565.
Chen, X., Macica, C., Nasiri, A., Judex, S. and Broadus, A. E. (2007). Mechanical regulation of PTHrP expression in entheses. *Bone* **41**, 752-759.
Chen, J., Sorensen, K. P., Gupta, T., Kilts, T., Young, M. and Wadhwa, S. (2009). Altered functional loading causes differential effects in the subchondral bone and condylar cartilage in the temporomandibular joint from young mice. *Osteoarthritis Cartilage* **17**, 354-361.
Deymier-Black, A. C., Singhal, A., Yuan, F., Almer, J. D., Brinson, L. C. and Dunand, D. C. (2013). Effect of high-energy X-ray irradiation on creep mechanisms in bone and dentin. *J. Mech. Behav. Biomed. Mater.* **21**, 17-31.
Galatz, L., Rothermich, S., VanderPloeg, K., Petersen, B., Sandell, L. and Thomopoulos, S. (2007). Development of the supraspinatus tendon-to-bone insertion: localized expression of extracellular matrix and growth factor genes. *J. Orthop. Res.* **25**, 1621-1628.
Grimsrud, C. D., Romano, P. R., D'Souza, M., Puzas, J. E., Schwarz, E. M., Reynolds, P. R., Roiser, R. N. and O'Keefe, R. J. (2001). BMP signaling stimulates chondrocyte maturation and the expression of Indian hedgehog. *J. Orthop. Res.* **19**, 18-25.
Hilton, M. J., Tu, X. and Long, F. (2007). Tamoxifen-inducible gene deletion reveals a distinct cell type associated with trabecular bone, and direct regulation of PTHrP expression and chondrocyte morphology by Ihh in growth region cartilage. *Dev. Biol.* **308**, 93-105.
Hojo, H., Ohba, S., Taniguchi, K., Shirai, M., Yano, F., Saito, T., Ikeda, T., Nakajima, K., Komiyama, Y., Nakagata, N. et al. (2013). Hedgehog-Gli activators direct osteo-chondrogenic function of bone morphogenetic protein toward osteogenesis in the perichondrium. *J. Biol. Chem.* **288**, 9924-9932.
Ingham, P. W. and McMahon, A. P. (2001). Hedgehog signaling in animal development: paradigms and principles. *Genes Dev.* **15**, 3059-3087.
Kobayashi, T., Soegiarto, D. W., Yang, Y., Lanske, B., Schipani, E., McMahon, A. P. and Kronenberg, H. M. (2005). Indian hedgehog stimulates periarticular chondrocyte differentiation to regulate growth plate length independently of PTHrP. *J. Clin. Invest.* **115**, 1734-1742.
Kovacevic, D. and Rodeo, S. A. (2008). Biological augmentation of rotator cuff tendon repair. *Clin. Orthop. Relat. Res.* **466**, 622-633.
Kronenberg, H. M. (2003). Developmental regulation of the growth plate. *Nature* **423**, 332-336.
Lai, L. P. and Mitchell, J. (2005). Indian hedgehog: its roles and regulation in endochondral bone development. *J. Cell. Biochem.* **96**, 1163-1173.
Lanske, B., Karaplis, A. C., Lee, K., Luz, A., Vortkamp, A., Pirro, A., Karperien, M., Defize, L. H. K., Ho, C., Mulligan, R. C. et al. (1996). PTH/PTHrP receptor in early development and Indian hedgehog–regulated bone growth. *Science* **273**, 663-666.
Legros, R., Balmain, N. and Bonel, G. (1987). Age-related changes in mineral of rat and bovine cortical bone. *Calcif. Tissue Int.* **41**, 137-144.
Liu, C.-F., Aschbacher-Smith, L., Barthelery, N. J., Dyment, N., Butler, D. and Wylie, C. (2012). Spatial and temporal expression of molecular markers and cell signals during normal development of the mouse patellar tendon. *Tissue Eng. Part A* **18**, 598-608.
Liu, C.-F., Breidenbach, A., Aschbacher-Smith, L., Butler, D. and Wylie, C. (2013). A role for hedgehog signaling in the differentiation of the insertion site of the patellar tendon in the mouse. *PLoS ONE* **8**, e65411.
Long, F. and Ornitz, D. M. (2013). Development of the endochondral skeleton. *Cold Spring Harb. Perspect. Biol.* **5**, a008334.
Long, F., Zhang, X. M., Karp, S., Yang, Y. and McMahon, A. P. (2001). Genetic manipulation of hedgehog signaling in the endochondral skeleton reveals a direct role in the regulation of chondrocyte proliferation. *Development* **128**, 5099-5108.
Long, F., Chung, U.-i., Ohba, S., McMahon, J., Kronenberg, H. M. and McMahon, A. P. (2004). Ihh signaling is directly required for the osteoblast lineage in the endochondral skeleton. *Development* **131**, 1309-1318.
Lu, H. H. and Thomopoulos, S. (2013). Functional attachment of soft tissues to bone: development, healing, and tissue engineering. *Annu. Rev. Biomed. Eng.* **15**, 201-226.
Miller, L. M., Vairavamurthy, V., Chance, M. R., Mendelsohn, R., Paschalis, E. P., Betts, F. and Boskey, A. L. (2001). In situ analysis of mineral content and crystallinity in bone using infrared micro-spectroscopy of the nu(4) PO(4)(3-) vibration. *Biochim. Biophys. Acta* **1527**, 11-19.
Minina, E., Wenzel, H. M., Kreschel, C., Karp, S., Gaffield, W., McMahon, A. P. and Vortkamp, A. (2001). BMP and Ihh/PTHrP signaling interact to coordinate chondrocyte proliferation and differentiation. *Development* **128**, 4523-4534.
Muzumdar, M. D., Tasic, B., Miyamichi, K., Li, L. and Luo, L. (2007). A global double-fluorescent Cre reporter mouse. *Genesis* **45**, 593-605.
Ng, T. C. S, Chiu, K. W. K., Rabie, A. B. M. and Hägg, U. (2006). Repeated mechanical loading enhances the expression of Indian hedgehog in condylar cartilage. *Front. Biosci.* **11**, 943-948.
Nowlan, N. C., Prendergast, P. J. and Murphy, P. (2008). Identification of mechanosensitive genes during embryonic bone formation. *PLoS Comput. Biol.* **4**, e1000250.
Schneider, C. A., Rasband, W. S. and Eliceiri, K. W. (2012). NIH Image to ImageJ: 25 years of image analysis. *Nat. Methods* **9**, 671-675.
Schwartz, A. G., Pasteris, J. D., Genin, G. M., Daulton, T. L. and Thomopoulos, S. (2012). Mineral distributions at the developing tendon enthesis. *PLoS ONE* **7**, e48630.
Schwartz, A. G., Lipner, J. H., Pasteris, J. D., Genin, G. M. and Thomopoulos, S. (2013). Muscle loading is necessary for the formation of a functional tendon enthesis. *Bone* **55**, 44-51.
Seidel, K., Ahn, C. P., Lyons, D., Nee, A., Ting, K., Brownell, I., Cao, T., Carano, R. A. D., Curran, T., Schober, M. et al. (2010). Hedgehog signaling regulates the generation of ameloblast progenitors in the continuously growing mouse incisor. *Development* **137**, 3753-3761.
Shao, Y. Y., Wang, L., Welter, J. F. and Ballock, R. T. (2012). Primary cilia modulate Ihh signal transduction in response to hydrostatic loading of growth plate chondrocytes. *Bone* **50**, 79-84.
Shin, K., Lee, J., Guo, N., Kim, J., Lim, A., Qu, L., Mysorekar, I. U. and Beachy, P. A. (2011). Hedgehog/Wnt feedback supports regenerative proliferation of epithelial stem cells in bladder. *Nature* **472**, 110-114.
Silva, M. J., Thomopoulos, S., Kusano, N., Zaegel, M. A., Harwood, F. L., Matsuzaki, H., Havlioglu, N., Dovan, T. T., Amiel, D. and Gelberman, R. H. (2006). Early healing of flexor tendon insertion site injuries: tunnel repair is mechanically and histologically inferior to surface repair in a canine model. *J. Orthop. Res.* **24**, 990-1000.
St-Jacques, B., Hammerschmidt, M. and McMahon, A. P. (1999). Indian hedgehog signaling regulates proliferation and differentiation of chondrocytes and is essential for bone formation. *Genes Dev.* **13**, 2072-2086.
Sugimoto, Y., Takimoto, A., Akiyama, H., Kist, R., Scherer, G., Nakamura, T., Hiraki, Y. and Shukunami, C. (2013). Scx+/Sox9+ progenitors contribute to the establishment of the junction between cartilage and tendon/ligament. *Development* **140**, 2280-2288.
Thomopoulos, S., Hattersley, G., Rosen, V., Mertens, M., Galatz, L., Williams, G. R. and Soslowsky, L. J. (2002). The localized expression of extracellular matrix components in healing tendon insertion sites: an in situ hybridization study. *J. Orthop. Res.* **20**, 454-463.
Thomopoulos, S., Kim, H.-M., Rothermich, S. Y., Biederstadt, C., Das, R. and Galatz, L. M. (2007). Decreased muscle loading delays maturation of the tendon enthesis during postnatal development. *J. Orthop. Res.* **25**, 1154-1163.
Thomopoulos, S., Genin, G. M. and Galatz, L. M. (2010). The development and morphogenesis of the tendon-to-bone insertion - what development can teach us about healing. *J. Musculoskelet. Neuronal Interact.* **10**, 35-45.
Voehringer, D., Liang, H.-E. and Locksley, R. M. (2008). Homeostasis and effector function of lymphopenia-induced "memory-like" T cells in constitutively T cell-depleted mice. *J. Immunol.* **180**, 4742-4753.
Vortkamp, A., Lee, K., Lanske, B., Segre, G. V., Kronenberg, H. M. and Tabin, C. J. (1996). Regulation of rate of cartilage differentiation by Indian hedgehog and PTH-related protein. *Science* **273**, 613-622.
Vortkamp, A., Pathi, S., Peretti, G. M., Caruso, E. M., Zaleske, D. J. and Tabin, C. J. (1998). Recapitulation of signals regulating embryonic bone formation during postnatal growth and in fracture repair. *Mech. Dev.* **71**, 65-76.
Wang, I.-N. E., Mitroo, S., Chen, F. H., Lu, H. H. and Doty, S. B. (2006). Age-dependent changes in matrix composition and organization at the ligament-to-bone insertion. *J. Orthop. Res.* **24**, 1745-1755.
Wang, Y., Zhou, Z., Walsh, C. T. and McMahon, A. P. (2009). Selective translocation of intracellular Smoothened to the primary cilium in response to Hedgehog pathway modulation. *Proc. Natl. Acad. Sci. USA* **106**, 2623-2628.
Wang, M., VanHouten, J. N., Nasiri, A. R., Johnson, R. L. and Broadus, A. E. (2013). PTHrP regulates the modeling of cortical bone surfaces at fibrous insertion sites during growth. *J. Bone Miner. Res.* **28**, 598-607.
Wu, Q.-q, Zhang, Y. and Chen, Q. (2001). Indian hedgehog is an essential component of mechanotransduction complex to stimulate chondrocyte proliferation. *J. Biol. Chem.* **276**, 35290-35296.
Zhao, H., Feng, J., Seidel, K., Shi, S., Klein, O., Sharpe, P. and Chai, Y. (2014). Secretion of shh by a neurovascular bundle niche supports mesenchymal stem cell homeostasis in the adult mouse incisor. *Cell Stem Cell* **14**, 160-173.